A Novel MAC Protocol Exploiting Concurrent Transmissions for Massive LoRa Connectivity

Yujun Hou, Zujun Liu, and Dechun Sun

Abstract: **Among variant low-power wide area networks (LPWAN), LoRa is one of the most promising and is extensively deployed worldwide because of its satisfactory performance and relatively low cost. In the foreseen future, various internet of things (IoT) applications are required to sustain connectivity for massive end-devices. Massive connectivity challenges the LoRaWAN network based on ALOHA medium access control (MAC) protocol due to severe collisions under high traffic loads. To solve this problem, we first dissect the principles and characteristics of LoRa physical layer. And it suggests that the capture effect among the signals with the same spreading factor (SF) and different SFs can be adequately leveraged to improve performance. Based on the capture effect, we develop a new receiver structure that enables the superposed LoRa signals with different odd/even SFs to be demodulated simultaneously. A suitable novel MAC protocol exploiting such concurrent transmissions is further presented. Simulations verify that, through utilizing the capture effect, the proposed protocol can partly tackle the collisions due to numerous access attempts, which results in enhancing the throughput compared to LoRaWAN. These results show that the proposed scheme is compliant with the requirement of IoT applications with massive connectivity.**

Index Terms: **Capture effect, LoRa, low-power wide area networks (LPWAN), massive connectivity, medium access control (MAC).**

I. INTRODUCTION

THE design target of low-power wide area networks (LPWAN) [1] lies in providing and sustaining a long range communication of massive low-cost internet of things (IoT) devices with ultra-low power consumptions. LoRa [2] as one of the most promising technologies, utilizes the chirp spread spectrum (CSS) technique to allow the receivers to decode signals with a relatively low sensitivity. The data rate and the communication range of LoRa can vary through selecting different spreading factors (SFs). Operating on sub-GHz band and respecting the local transmit duty cycle regulations, the LoRa signals suffer from less attenuation and congestions. To extend the battery life, the end-devices only wake up from sleep state periodically or when triggered by events. By reducing hardware complexity and applying the license-free bands, LoRa can lower establishment and deployment cost, which is the key to the commercial success. Standardized and generalized by the LoRa Alliance, LoRaWAN [3] bases on pure ALOHA medium access control (MAC) protocol and defines the MAC layer and above.

In general, IoT application scenarios can be divided into two categories [4]. One is critical IoT that demands high reliability and low latency, including scenarios such as smart health care, smart transportation, and smart manufacturing. The other is massive IoT (mIoT) that is characterized by massive access devices and latency tolerance. In a mIoT scenario, like smart grids and smart agriculture, a base-station or a gateway potentially manages 10^4–10^6 devices [5]. Although the traffic pattern of the devices is sporadic, it may arise severe collisions and congestions when so many devices attempt to access. Thus, massive connectivity is a crucial requirement for the future wireless network to support the mIoT. To overcome the noticeable performance degradation due to massive IoT access, many techniques have been presented for cellular IoT network recently. The first class of solutions is conducted at physical layer (PHY), such as employing compressed sensing technique to detect active users and estimate channel [6], [7], designing non-orthogonal pilots [8], and using non-orthogonal multiple access [9]. With regard to MAC layer, some works advocate modifying ALOHA and creating new protocols, like hint protocol [10]. Furthermore, combining the PHY multi-packet reception capability with the MAC protocol design [11], a drastic performance augment can always be produced. Most solutions share a common that they call for the usage of grant-free random access strategies , i.e., an active device transmits metadata and payload directly without any access requirement. Grant-free strategies not only decrease the access latency but also abate the total number of packets and the power consumption on overhead, so that it is of vital importance in an IoT massive connectivity scenario [12], [13].

Employing the grant-free strategy, LoRaWAN is possible to be applied to the mIoT. Due to massive IoT access attempts, however, there are numerous concurrent transmissions in the LoRa networks, which may cause the co-SF interference among the end-devices with an identical SF and the inter-SF interference among the end-devices with distinct SFs [14]. As for ALOHA-based LoRaWAN, such interference is more inevitable. Besides, the duty cycle regulations, retransmissions, acknowledgments, and downlink messages will also bring about heavy congestions and collisions. In the end, the coverage and the throughput performance of LoRaWAN drop exponentially as the number of the end-devices and the traffic loads increases [15], [16]. Fortunately, thanks to its unique modulation scheme, LoRa has a phenomenon referred to the capture effect [17], [18] that the reception can succeed even in the presence of the co-SF and the inter-SF interference provided its signal-to-interference-plus-noise ratio (SINR) exceeds the cor-

Manuscript received August 26, 2019; Revised December 31, 2019; approved for publication by Ruonan Zhang, Division II Editor.

This work was supported in part by the National Natural Science Foundation of China under Grant 61571340.

Y. Hou, Z.Liu, and D. Sun are with the State Key Laboratory of Integrated Services Networks, Xidian University, Xi'an, 710071, China, e-mail: houyujunyl@163.com, {liuzujun, dcsun}@mail.xidian.edu.cn.

Z. Liu is the corresponding author.

Digital Object Identifier: 10.1109/JCN.2020.000005

responding threshold. A signal with the co-SF interference can be captured and decoded successfully if its power is at least 6 dB stronger than that of any other [19], [20]. Furthermore, confirmed by the measurement studies, simulations, and mathematical analyzes [14], [21], [22], it is explicit that the LoRa signals with different SFs are quasi-orthogonal to each other, which are considered perfectly orthogonal previously. Therefore, it is feasible to utilize the capture effect to tackle the collisions in the LoRa networks [17], [23].

Up to now, some works devote to settling the problem through allocating frequency channels and SFs. Reference [24] has investigated the conditions for the gateway correctly decoding the packets, and then optimized the average system packet success probability by allocating SFs to achieve maximum connectivity. Reference [25] has raised a two-step light-weight scheduling to group the end-devices based on the allowable power and SFs. Particularly, the author try to mitigate the capture effect, which is thought to be destructive to the end-devices far from the gateway on account of losing the transmission opportunity. More recent attentions have focused on improving the existing MAC protocol of LoRaWAN. An original PHY decoding scheme and MAC protocol are presented in [26], in which the slight desynchronization of the superposed signals is exploited. Nevertheless, the proposed MAC protocol does not consider the LoRa capture effect and is limited by the noise. The method in [27] makes use of carrier sense multiple access (CSMA) to achieve the less collision ratio and the higher throughput while the energy consumption slightly increases. However, it does not take the hiding-nodes effect into consideration. The study on [28] has put forward that LoRaWAN performance can be augmented with the listen before talk (LBT) scheme. Concerning the real-time flow in Industry 4.0 applications, [29] has introduced a random access strategy–Industrial LoRa–to support periodic real-time traffic and aperiodic traffic.

To mitigate the congestions and collisions due to massive connectivity in the LoRa networks, the key contributions of the paper are two-fold as follows:

i) By exploiting the capture effect, we design a novel receiver structure based on oversampling so as to enable three superposed signals with different odd/even SFs to be demodulated simultaneously with a single fast Fourier transform (FFT) module. Compared to the traditional receiver [19], the proposed receiver achieves a higher demodulation efficiency and a lower complexity in the concurrent transmissions situation.

ii) We develop a new MAC protocol based on the proposed receiver structure, in which the packets with distinct odd/even SFs are obliged to transmit concurrently. More interfered packets can fulfill the capture conditions, and simulations show that the proposed protocol is able to significantly reduce the packet collision ratio and enhance the network throughput compared to the conventional LoRaWAN.

The rest of this paper is organized as follows. The LoRa PHY modulation scheme, the capture effect, and the LoRaWAN overview are presented in Section II. In Section III, the principle of the novel receiver structure is introduced. The proposed MAC protocol is specified in Section IV. Section V shows the results simulated in MATLAB for the bit error ratio (BER) performance and in the discrete event simulator NS-3 for MAC protocol evaluation. Finally, Section VI draws the conclusions.

II. OVERVIEW OF LORA PHY AND LORAWAN

LoRa is a proprietary PHY layer technique possessed by Semtech Corporation, and LoRaWAN is the MAC layer protocol specified by LoRa Alliance. In the following, they are outlined.

A. LoRa PHY

To cope with the requirements of IoT, the CSS modulation in LoRa is evolved and combined with the high-order M-ary frequency shift keying (FSK) [17], [30]. Supposing that the LoRa chirp spreads in a bandwidth B, one LoRa sample is then transmitted every $T_C = 1/B$. Each LoRa symbol consists of 2^{SF} samples, therefore, the total symbol duration is $T_S = 2^{SF} \times T_C$. Every SF binary bits is encoded and mapped to a unique non-binary symbol $s_p = p$, where $p \in \{0, 1, \cdots, 2^{SF} - 1\}$ [19], [31]. By cyclically shifting the raw up-chirp, the value of p exclusively determines the initial frequency $f_{cc}(0) = (B \times p)/2^{SF}$ of the modulated chirp [19]. Accordingly, the instantaneous frequency of the LoRa modulated chirp is expressed as:

$$f_{cc}(k) = \begin{cases} \frac{B \times (k+p)}{2^{SF}}, & 0 \le k \le 2^{SF} - p, \\ \frac{B \times (k+p)}{2^{SF}} - B, & 2^{SF} - p \le k \le 2^{SF} - 1. \end{cases} \tag{1}$$

It appears a sharp edge in spectrum, where the value of the instantaneous frequency at the transition changes fiercely from B to 0. Let us assume that the initial phase of the coded chirp is 0. Based on (1) and the relation between the instantaneous frequency and the phase, the LoRa modulated chirp symbol can be written by:

$$c_p(k) = \exp\left[j\pi \frac{(k^2 + 2pk)}{2^{SF}}\right]. \tag{2}$$

At the receiver, the LoRa demodulation starts firstly by a dechirping step that the received signal is multiplied by the raw down-chirp [31]. Secondly, 2^{SF} points FFT is performed on the de-chirped signal. As long as the signal-to-noise ratio (SNR) is great enough, the index with the highest magnitude indicates the the encoded symbol s_p [32].

To further increase the robustness to interference, data whitening, interleaving, forward error correction, and gray indexing techniques are applied before the LoRa modulation [30]. Thus, the bit rate $R_b = SF \times (B/2^{SF}) \times 4/(4 + CR)$ bits/s, where $CR \in \{1, 2, 3, 4\}$ is the code rate. Thanks to the processing gain $G_p = 10 \log\left(2^{SF}/SF\right)$ [30], LoRa can obtain a good link budget and readily achieve a long transmission distance for several kilometers.

The LoRa capture effect refers to the phenomenon that a desired signal suffering from interference can be decoded correctly if its SINR exceeds the corresponding threshold. The LoRa capture effect is primarily reliant on the orthogonality, i.e., the LoRa symbols with identical SF and bandwidth but different initial frequencies are perfectly orthogonal [33]; the

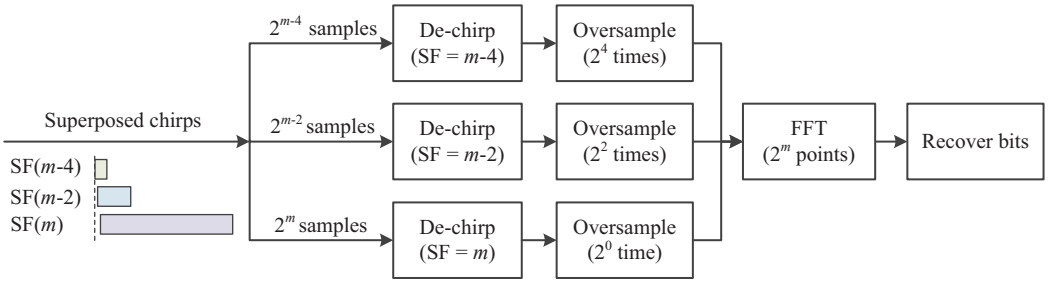

Fig. 1. Proposed PHY receiver structure based on the capture effect. $m = 11$ for the odd-SF subset and $m = 12$ for the even-SF subset.

LoRa symbols with same bandwidth but different SFs are quasi-orthogonal [18], [34]. Accordingly, the co-SF and inter-SF capture conditions must be fulfilled to decode the desired signal [14], [22], which can be given by:

$$SINR_{ij} = \frac{P_i}{P_j + \sigma^2} \geq q_{ij}, \tag{3}$$

where P_i and P_j ($i, j \in \{7, 8, \cdots, 12\}$) are the power of the desired and the interfering symbol, respectively, σ^2 is the channel noise power, and q_{ij} is the required threshold.

Based on the analyzes in [17], [20], a threshold of 6 dB is reasonable for identifying the maximum magnitude of the desired LoRa symbol with co-SF interference. The symbols with different SFs are imperfectly orthogonal, so the residual inter-SF interference cannot be ignored, particularly when the interfering end-device is much closer to the gateway than the desired one. Confirmed by the simulations and the experiments in [21], [34], the inter-SF threshold is SF-specific and is much smaller than 0 dB.

B. LoRaWAN

With a star topology, the gateway in a LoRa network transparently relays information between the end-devices and the network server. All communication is bi-directional, while the uplink communication is dominant in most application scenarios. The LoRaWAN specification [3] suggests that we can trade data rate (DR) for communication distance through selecting alternative SFs and bandwidths. All end-devices and gateways must obey the local duty cycle regulations or apply LBT scheme so as to cut down the total number of packets in the network and be compatible of the other existing networks.

LoRaWAN specifies a basic device Class A and two optional Class B and C. In Class A, the communication is initiated by the end-devices using ALOHA mechanism. The downlink data is only permitted soon after a successful uplink transmission. The end-devices in Class B increase more receive windows in scheduled times, besides the windows in Class A. So the gateway must send beacons periodically as a synchronization reference. A Class C end-device is always available for reception, except for the transmitting period. Accordingly, Class A is suitable for energy-constrained end-devices, whilst Class B or C should be utilized in delay-sensitive applications.

III. NOVEL RECEIVER STRUCTURE

In the light of the latest SX1301 gateway [19], [35], a single FFT module is only able to demodulate an SF-specific LoRa signal at any time. So it may be difficult for the traditional LoRa gateway to handle the many access attempts in the mIoT. In order to further improve the throughput of the LoRa gateway, we design a novel receiver structure exploiting the capture effect described above.

The idea of the proposed receiver structure is to make the superposed chirp symbols with different SFs have the same number of samples by oversampling. So they can be decoded simultaneously using a single FFT module. According to the inter-SF quasi-orthogonality, the superposed chirp symbols have a good cross-correlation and can be decoded correctly given a sufficient SINR. For a fixed bandwidth, the inter-SF interference to the desired signal is more intense when it collides with a signal having a closer SF [21]. Furthermore, a lower SIR threshold for an acceptable BER is required while the interfering SF is greater. Therefore, in the proposed receiver, SF7–SF12 are divided into two subsets: the odd-SF subset $\mathbb{SF}_o = \{7, 9, 11\}$ and the even-SF subset $\mathbb{SF}_e = \{8, 10, 12\}$. Three LoRa signals with different SFs in the same subset are allowed to transmit concurrently on the same channel.

The proposed receiver structure is depicted in Fig. 1. We assume that the end-devices are synchronized and the chirp symbols that belong to the same subset arrive at the gateway at the same time. Let us denote SF(m) as the maximum SF in $\mathbb{SF}_o$ or $\mathbb{SF}_e$. Accordingly, the SFs of the other two superposed symbols are SF($m-2$) and SF($m-4$). Thus, the received signal is:

$$\begin{aligned} y(k) &= c_{m-4,p}(k) + c_{m-2,q}(k) + c_{m,r}(k) \\ &= \sum_{k=0}^{2^{m-4}-1} e^{j\pi \frac{k^2+2pk}{2^{m-4}}} + \sum_{k=0}^{2^{m-2}-1} e^{j\pi \frac{k^2+2qk}{2^{m-2}}} \\ &\quad + \sum_{k=0}^{2^{m}-1} e^{j\pi \frac{k^2+2rk}{2^{m}}}, \end{aligned} \tag{4}$$

where p, q, and r are the corresponding non-binary encoded symbols. To demodulate the desired chirp symbol with SF($m-4$), the received signal should firstly be multiplied by

the raw down-chirp, so the de-chirped signal is:

$$dy_{m-4,p}(k) = \sum_{k=0}^{2^{m-4}-1} y(k) \times e^{-j\pi \frac{k^2}{2^{m-4}}} = \sum_{k=0}^{2^{m-4}-1} e^{j\pi \frac{2pk}{2^{m-4}}} + I(k), \quad (5)$$

where $I(k)$ indicates the negative impact of SF($m-2$) and SF(m).

Then, the de-chirped signal should be oversampled by $N = 2^{m-(m-4)} = 2^4$ times. The oversampling outputs are given by:

$$v_{m-4,p}(l) = \begin{cases} dy_{m-4,p}(\frac{l}{N}), & l = 0, N, \cdots, (2^{m-4}-1)N, \\ 0, & \text{otherwise}, \end{cases} = \begin{cases} \sum_{l=0}^{2^m-1} e^{j\frac{2\pi pl}{2^m}} + I'(l), & l = 0, N, \cdots, (2^{m-4}-1)N, \\ 0, & \text{otherwise}. \end{cases} \quad (6)$$

After oversampling, all three chirp symbols from the same subset possess 2^m samples. So an identical FFT module with 2^m points can be applied to the signals after oversampling. The FFT outputs can be written by:

$$X_{m-4,p}[n] = \text{FFT}[v_{m-4,p}(l)]|_{2^m} = \sum_{l=0}^{2^m-1} v_{m-4,p}(l) \times e^{-j\frac{2\pi l}{2^m}n} = \sum_{l=0}^{2^m-1} e^{j\frac{2\pi l}{2^m}(p-n)} + I^*(n), \quad (7)$$

where $n = 0, 1, \cdots, 2^m - 1$, and $I^*(n)$ refers to the the residual interference from the chirps with SF($m-2$) and SF(m). Noting that the result of (7) is equal to zero when $l \neq 0, N, \cdots, (2^{m-4}-1)N$. Accordingly, the magnitudes of the FFT outputs can be calculated as:

$$|X_{m-4,p}(n)| = \begin{cases} |2^m + I^*(n)|, & n = p, 2p, \cdots, Np, \\ |I^*(n)|, & n \neq p, 2p, \cdots, Np. \end{cases} \quad (8)$$

Considering a sufficient SIR, the magnitudes at indices $n = p, 2p, \cdots, Np$ outstand with the same value. Consequently, by distinguishing the highest magnitude from the first 2^{m-4} indices, the $(m-4)$ binary bits can be recovered. To demodulate the chirp symbol with SF($m-2$) or SF(m), the three same steps: de-chirping, oversampling, and performing 2^m points FFT should be followed as shown in Fig. 1.

Taking $m = 11$ as an example, i.e., the SFs of the desired symbols are in the odd-SF subset $\mathbb{SF}_o$. The normalized magnitudes of the FFT outputs are illustrated in Fig. 2. Interestingly, the FFT outputs appear 2^4 peaks with the same magnitude for SF7, 2^2 peaks for SF9, and 2^0 peaks for SF11.

Taking advantage of the LoRa capture effect, the three synchronized LoRa signals can be decoded simultaneously. Moreover, only one single FFT module is employed to demodulate the signals with odd/even SFs through utilizing the oversampling. So the receiver complexity can be reduced. When the interference has a random delay, the desired signal can still be received with a relatively low SINR threshold [34]. Thus, the proposed receiver structure is also robust to the timing offset.

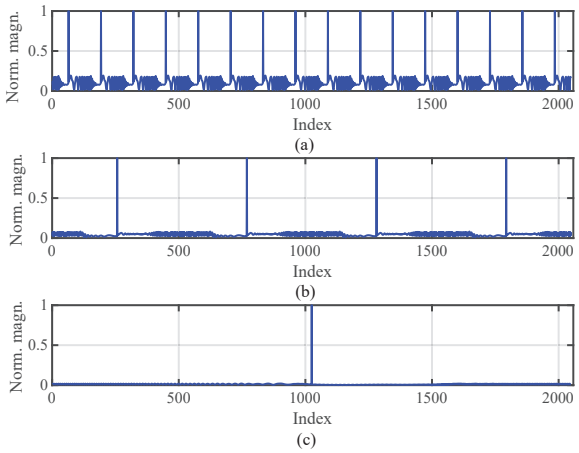

Fig. 2. Normalized magnitudes of the FFT outputs ($m = 11$) with $s_p = 2^{SF_{des}-1}$: (a) $SF_{des} = 7$, (b) $SF_{des} = 9$, and (c) $SF_{des} = 11$.

IV. MAC PROTOCOL EXPLOITING CONCURRENT TRANSMISSIONS

For most mIoT applications, the traffic size is small and the traffic pattern is sporadic. Moreover, the transmissions of the end-devices are limited due to the duty cycle regulation. As the number of end-devices and traffic loads increases, however, the LoRa signals are highly possible to suffer from both the co-SF and the inter-SF interference. Without any collision avoidance scheme, the traditional ALOHA-based LoRaWAN may turn into saturation rapidly and arise severe congestions.

To fulfill the requirement of massive connectivity, in addition to the proposed receiver structure, we develop a MAC protocol referred to capture effect-MAC (CE-MAC), which is also a grant-free random access scheme. In this way, the handshakes can be reduced in the connection establishment between the end-devices and the gateway, which abates the collisions and the access delay [12], [13]. To exploit the capture effect to further mitigate the collisions, the CE-MAC protocol enables three synchronized LoRa frames with different odd/even SFs to transmit concurrently.

In order to synchronize the end-devices in the network, the gateway is scheduled to send beacons periodically. Upon receiving a beacon, an end-device can start transmitting frames. All end-devices should have a synchronous timing-slot, but a perfectly synchronization at symbol or block symbol is unnecessary, as shown in Fig. 3. The Odd_Slot is dedicate for the odd-SF transmissions and the Even_Slot is for the even-SF transmissions. Additionally, an Odd_Slot and Even_Slot are composed of a set of the Odd_Subslots and the Even_Subslots possessing a shorter time period. A LoRa frame may occupy one or several subslots relying on its time on air (ToA).

Fig. 4 depicts the flow chart of the CE-MAC protocol. Each Odd_Slot and Even_Slot contain S subslots aligned from 0 to

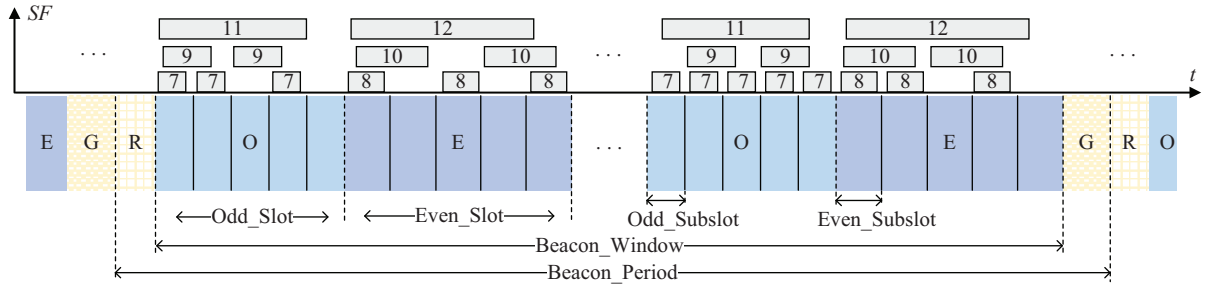

Fig. 3. Transmissions in the proposed CE-MAC protocol. A beacon frame can be divided into several Odd_Slots and Even_Slots. "G", "R", "O", and "E" stand for Beacon_Guard, Beacon_Reserved, Odd_Slot, and Even_Slot, respectively.

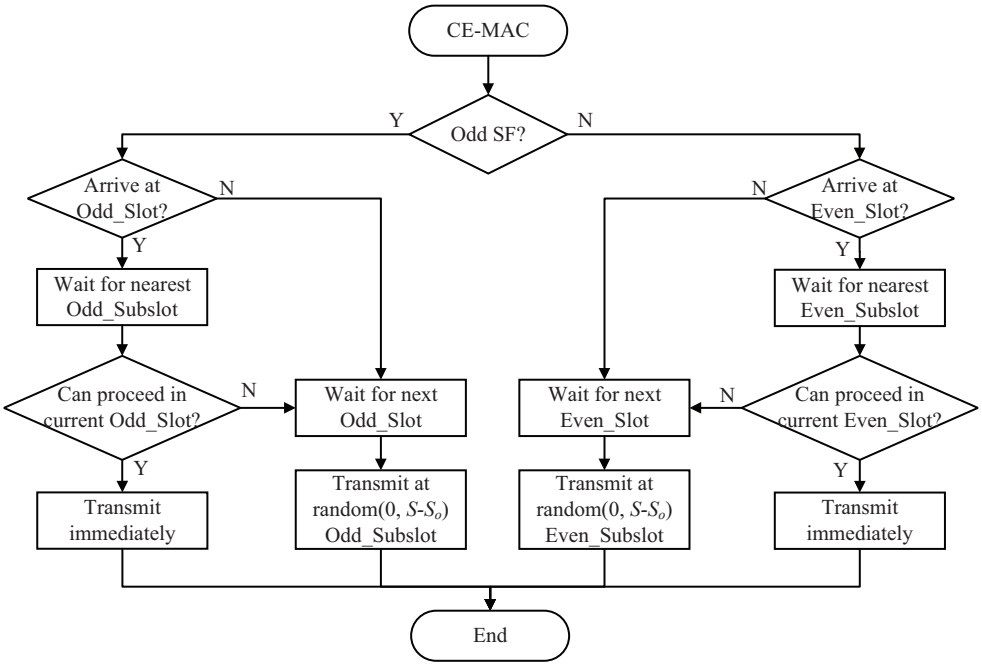

Fig. 4. Proposed CE-MAC protocol. A slot contains S subslots and the frame occupies $S_o(S_o \leq S)$ subslots.

$(S-1)$. Taking an odd-SF frame occupying $S_o(S_o \leq S)$ subslots as an example, we describe how the CE-MAC protocol works. When the frame arrives, the MAC layer should firstly evaluate whether it can be proceeded in the current slot. If it arrives at an Odd_Slot and there are $S_r(S_r \geq S_o)$ remaining Odd_Subslots, the frame can then be transmitted at the nearest upcoming number $(S - S_r)$ Odd_Subslot. As illustrated in Fig. 5, there exists four other cases that the frame cannot be proceeded immediately:

i) The frame arrives at an Odd_Slot but $S_r < S_o$, i.e., it cannot be proceeded at the current slot;
ii) The frame arrives at an Even_Slot;
iii) The frame arrives at the Beacon_Reserved;
iv) The frame arrives at the Beacon_Guard.

In these cases, the end-device must wait until the next Odd_Slot comes. Subsequently, the end-device will randomly select from the number 0 to the number $(S - S_o)$ Odd_Subslots to transmit the frame. Randomly selecting the Odd_Subslot can balance the traffic loads in the whole Odd_Slot. The even-SF frame in the CE-MAC protocol works in a similar way.

At the LoRa gateway, the reception condition is firstly check,

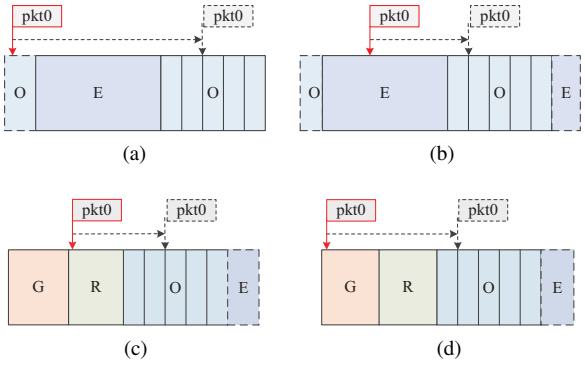

Fig. 5. Four cases that an odd-SF packet cannot be proceeded immediately: (a) The packet cannot be proceeded at Odd_Slot, (b) the packet arrives at Even_Slot, (c) the packet arrives at Because_Reserved, and (d) the packet arrives at Because_Guard.

i.e., the received power of the desired frame should exceed the receiver sensitivity. When it collides with other frames, the SINR of the desired frame should satisfy the co-SF and inter-SF capture conditions described in Section II. If these conditions are jointly fulfilled, the reception of the desired frame is success-

ful. Otherwise, the gateway cannot decode the frame correctly.

Exploiting the LoRa capture effect and the orthogonality, some collided frames may survive. In the CE-MAC protocol, the frames with odd/even SFs are scheduled to transmit concurrently. Compared to LoRaWAN, more frames in the CE-MAC protocol will satisfy the capture conditions. Consequently, more collisions can be resolved, which enables the grant-free CE-MAC protocol to address the massive LoRa connectivity problem. It is worth mentioning that, due to the great amount of end-devices, there exist Hidden Nodes and Exposed Nodes in the network. For the sake of reducing the handshakes and overheads for the massive LoRa connectivity, the problem is not taken into consideration, but it should be further studied in the future research.

V. SIMULATION RESULTS

To validate the performance of the proposed protocol, we run simulations on MATLAB and NS-3 platforms. The BER performance of our proposed receiver structure is presented and the capture threshold is renewed firstly. Subsequently, we compare the network performance for the proposed CE-MAC protocol with LoRaWAN. Finally, the CE-MAC protocol is applied to a smart city scenario.

A. PHY BER Performance

Because of the quasi-orthogonality among the LoRa signals with same bandwidth but different SFs, we will examine the residual interference and BER performance via the proposed receiver structure. In the simulations, one of the subset $\mathbb{SF}_o$ or $\mathbb{SF}_e$ is considered as the desired SF, so the other two are the interfering SFs. We assume that all received signals are with the same amplitude that is set to one, and the bandwidth B equals to 125 kHz.

The BER performance of the proposed receiver under AWGN channel are shown in Fig. 6. It can be apparently observed that the LoRa signals with smaller SFs suffer from slightly more severe BER degradation. The BER performance loss is around 1 dB for SF7 and 0.5 dB for SF8. While the signals with larger SFs, like SF11 and SF12, are nearly immune to such residual interference. This is due to the imperfect orthogonality have a greater impact on the symbols with smaller SF. Therefore, the superposed signals can be decoded via the proposed receiver with an acceptable BER performance. To compensate the loss of the small-SF packets, an appropriate SF allocation scheme [24] and message replication [36] can be employed.

We further identify the SIR thresholds required to decode the desired signals in the presence of the inter-SF interference. Assuming that the signal with the desired SF is partially collided by the signals with the other two interfering SFs in the same SF subset. There is a uniform random delay $\tau \in [-T_{Sint}, T_{Sint}]$ among the overlapped signals, where T_{Sint} is the symbol duration of the interfering signal. The amplitude of the desired signal is set to one, whilst that of the interferences rests with an adjustable SIR, namely $A_{int} = A_{des} \times \sqrt{10^{-SIR/10}}$.

For each desired signal, it can be recognized from the results in Fig. 7 that there is a SIR threshold below which the BER curve descends rapidly. In addition, the smaller the desired SF is, the higher the SIR threshold requires to demodulate. The SIR thresholds for all SFs are summarized in Table 1, which correspond to a BER of exceeding 10^{-2}.

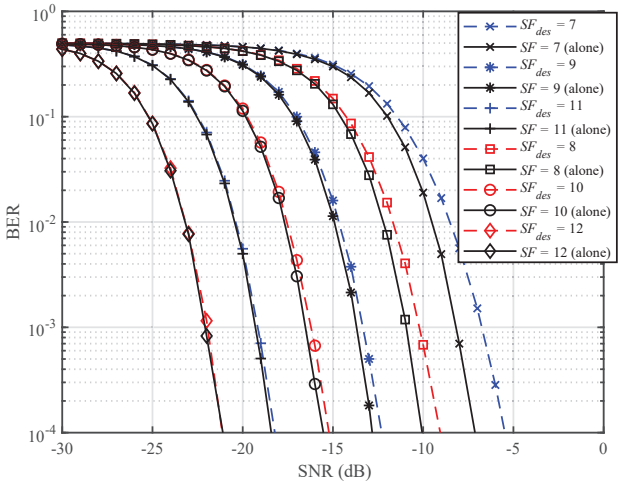

Fig. 6. BER performance of proposed receiver and traditional LoRa modulation under AWGN channel in function of SNR. $B = 125$ kHz, $CR = 0$.

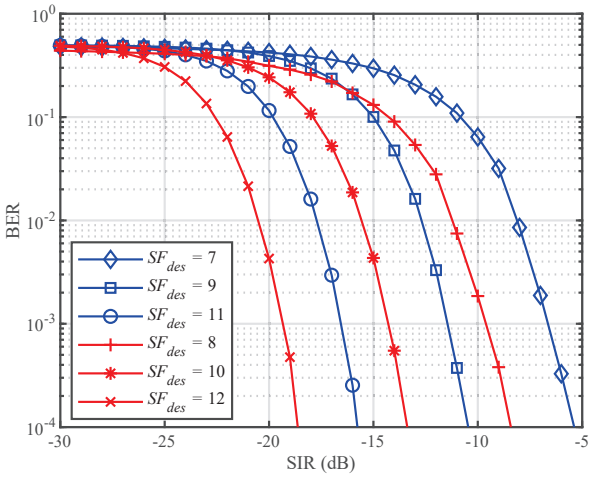

Fig. 7. BER of all SFs in function of SIR. $B = 125$ kHz, $CR = 0$.

Table 1. SIR thresholds for 3 Concurrent SFs. ($CR = 0$, $B = 125$ kHz).

SF combination	(7, 9, 11)			(8, 10, 12)		
Desired SF	7	9	11	8	10	12
SIR threshold (dB)	-7	-12	-17	-10	-15	-20

B. MAC Protocol Performance

In the simulations, the system has alterable number of the end-devices served by an individual gateway. The end-devices are randomly distributed around a circular area with a radius of 5 km, and the gateway locates at the center. The heights of the gateway and the end-devices are set to 30 m and 1 m above the ground, respectively.

In accordance with the measurement results in [37], the log-distance path loss model with shadow fading is given by:

$$PL(d)[dB] = \overline{PL}(d_0) + 10n \log\left(\frac{d}{d_0}\right) + X_\sigma, \qquad (9)$$

Table 2. DR0–DR5 on EU868 band.

DR	SF/B (1/kHz)	Bit rate (kb/s)	Receiver sensitivity (dBm)
0	12/125	0.29	137
1	11/125	0.54	134.5
2	10/125	0.98	132
3	9/125	1.76	129
4	8/125	3.13	126
5	7/125	5.47	123

Table 3. Simulation parameters.

Parameter	Value
Coding rate	1
Bandwidth	125 kHz
Transmission power	14 dBm
Preamble symbols	8
Number of channels	1
Channel frequency	868.1 MHz
Size of application payload	20 bytes
Arriving rate (Poisson)	1/900 s^{-1}

Table 4. Beacon and timing-slots configuration.

Parameter	Value
Beacon_Period	131,000 ms
Beacon_Reserved	2,000 ms
Beacon_Guard	3,000 ms
Beacon_Window	126,000 ms
Odd_Slot	864 ms
Even_Slot	1,656 ms
Odd_Subslot	72 ms
Even_Subslot	138 ms

where $\overline{PL}(d_0) = 128.95$ dB is the average path loss, $n = 2.32$ is the path loss exponent, d is the distance between transmitter and receiver, d_0 is the 1 km reference distance and X_σ is a Gaussian variable with zero mean, and $\sigma = 7.8$ dB is the standard deviation standing for a log-normal shadowing. The amount of the successfully delivered packets can exceed 80% under these parameter settings [37].

Based on the EU868 band [38] and the results in [15], [16], [28], the end-devices can randomly choose a mode from DR0-DR5 exhibited in Table 2. The simulation parameters herein are listed in Table 3. Considering the small packets and the sporadic traffic pattern features in the mIoT, the end-devices are set to send 20 byte messages generated following a Poisson process of rate $\lambda = 1/900$ s^{-1}. The ToAs of the frames with DR0-DR5 under such settings are 71.94 ms, 133.63 ms, 246.78 ms, 452.61 ms, 823.30 ms, and 1646.59 ms, respectively. Accordingly, the beacon and timing-slots are configured and are given in Table 4.

The inter-SF SIR thresholds in Table 1 and the 6 dB co-SF SIR threshold are utilized to model the LoRa orthogonality and the capture effect. The reception of a packet is regarded as failure if its received power is less than the given sensitivity. Moreover, we assume that a frame having the desired SF collapses when it is interfered by more than two SFs different from itself. The end-devices only transmit unconfirmed-data frames and the duty cycle is set to 1% and 0.1%.

Figs. 8 and 9 exhibit the packet delivery ratio (PDR) and the packet collision ratio (PCR) of LoRaWAN without/with capture effect and the CE-MAC protocol, respectively. The PDR is the ratio of the total number of the successful received packets to the

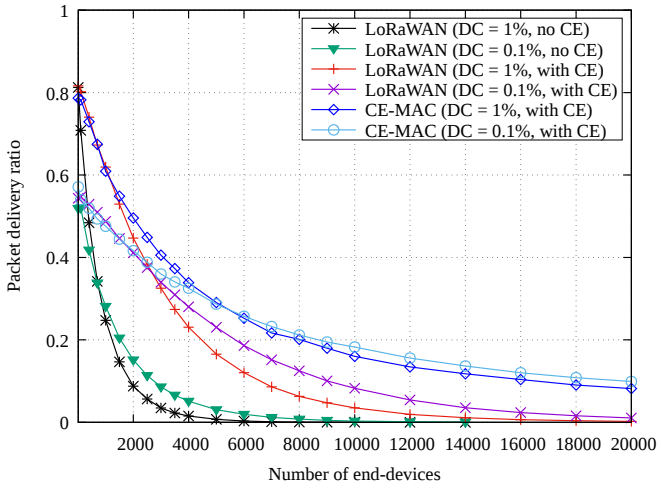

Fig. 8. Packet delivery ratio of LoRaWAN and CE-MAC in function of the number of end-devices. "DC" and "CE" stand for duty cycle and capture effect respectively.

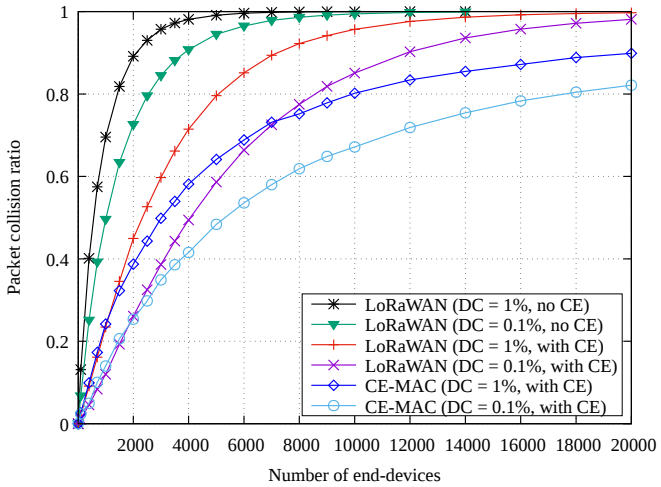

Fig. 9. Packet collision ratio of LoRaWAN and CE-MAC in function of the number of end-devices.

total number of the packets generated by all end-devices, with "1" as its unit. The PCR is the ratio of the total number of the discarded packets due to collisions to the total number of the packets successfully transmitted by all end-devices, with "1" as its unit.

It is observed that the PDRs of all protocols decrease as the number of end-devices scales up, while all the PCRs increase. These results imply that the network suffers from more serious congestions when more end-devices attempt to access. The performance of LoRaWAN with capture effect is better than LoRaWAN without capture effect. Without capture effect, a packet is considered as lost when a collision occurs. However, with the capture effect, the reception of a packet is successful as long as the capture condition is satisfied. The proposed CE-MAC protocol has the best performance. In the case of the network having 2×10^4 end-devices, the PCR of the CE-MAC is roughly 90% with 1% duty cycle and about 82% with 0.1% duty cycle, whilst the PCR of LoRaWAN is approximately 100%. In the CE-MAC protocol, the packets with odd/even SFs are transmitted concur-

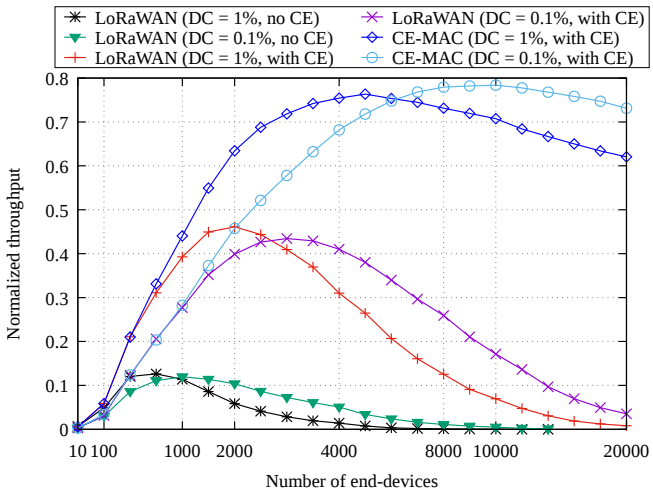

Fig. 10. Normalized throughput of LoRaWAN and CE-MAC in function of the number of end-devices.

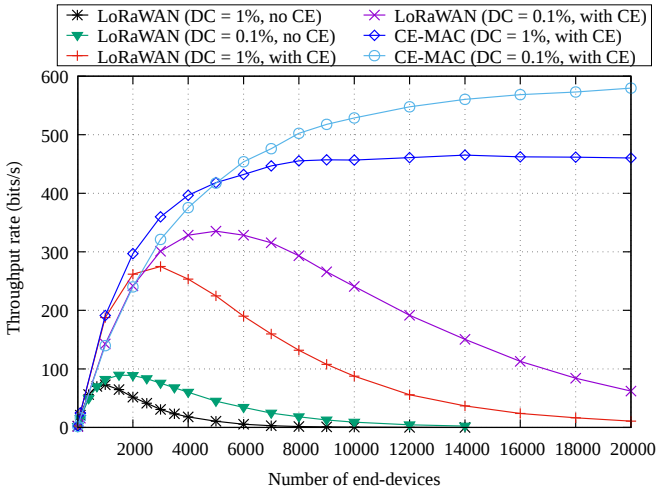

Fig. 11. Throughput rate of LoRaWAN and CE-MAC in function of the number of end-devices.

rently, and then more packets can be captured. Thus, the network can achieve a lower collision ratio. Furthermore, a lower duty cycle comes with a higher PDR and a lower PCR. This is because a lower duty cycle limits the transmissions of the end-devices, so the congestions and the collisions can be reduced.

Figs. 10 and 11 show the normalized throughput and the throughput rates of LoRaWAN without/with capture effect and the CE-MAC protocol, respectively. The normalized throughput equals to the ratio of the accumulated duration of successful received packets to the total simulation time, which is called link utilization ratio as well. The throughput rate equals to the ratio of the total bits successfully received by the gateway to the total simulation time, which is measured in bits/s.

We observe that the throughput of the CE-MAC protocol reaches the greatest saturation point compared with LoRaWAN without/with capture effect. The saturation point is related to the total arrive rate and the PCR of the LoRa network. LoRaWAN without capture effect supports the least end-devices when the network is saturated. Utilizing the capture effect can resolve partial collisions, so LoRaWAN with capture effect can support more end-devices. The CE-MAC achieves the lowest PCR, thus the network can attain saturation with the most end-devices. We also notice that the performance of LoRaWAN without/with capture effect degrades drastically as the number of end-devices further grows up to 2×10^4, while that of the CE-MAC protocol degrades much more slowly. This is due to the fact that, there exist some packets, especially the small-SF ones of shorter ToAs, can satisfy the capture condition and survive from the collisions in the CE-MAC. Again, we can see the impact of the duty cycle. The packet with smaller SF has a shorter ToA and a less probability of collisions, which results in a slightly enhancement in throughput rate. So the LoRa network with a lower duty cycle can support more end-devices.

Table 5. Hybrid traffic model.

Traffic rate	Proportion
1 pkt every 10 min per device	50%
1 pkt every 30 min per device	20%
1 pkt every 60 min per device	10%
Poisson with a 10 min traffic rate	20%

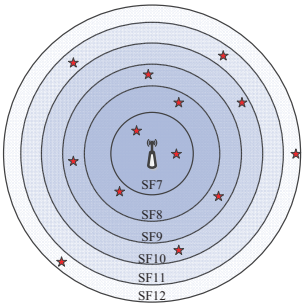

Fig. 12. SF allocation for EIB and EAB.

C. Smart City Case

In the following, the simulations are carried out to further apply the CE-MAC protocol and LoRaWAN to a smart city case [39], [40]. Accordingly, the end-devices are randomly distributed within a single gateway coverage with a radius of 1.2 km. We use the Okumura-Hata model plus a building penetration loss [41] to model the urban commercial environment. The smart city case includes many service sectors, such as smart governance, smart mobility, and smart buildings, and each might have a different traffic type. Therefore, based on the report in [39], a hybrid traffic model is considered as depicted in Table 5. Three SF allocation schemes are adopted as the following [24]:

i) Random scheme in which the end-devices can randomly choose SF.
ii) Equal-interval-based (EIB) scheme in which the end-devices choose SF by the doughnuts located, as illustrated in Fig. 12, and the intervals of doughnuts is equal.
iii) Equal-area-based (EAB) scheme in which the end-devices choose SF by the doughnuts located, and the areas of doughnuts are equal.

The other simulation parameters are the same as Tables 2, 3, and 4. The ducy cycle is set to 1% and the capture effect is taken into consideration for the two protocols.

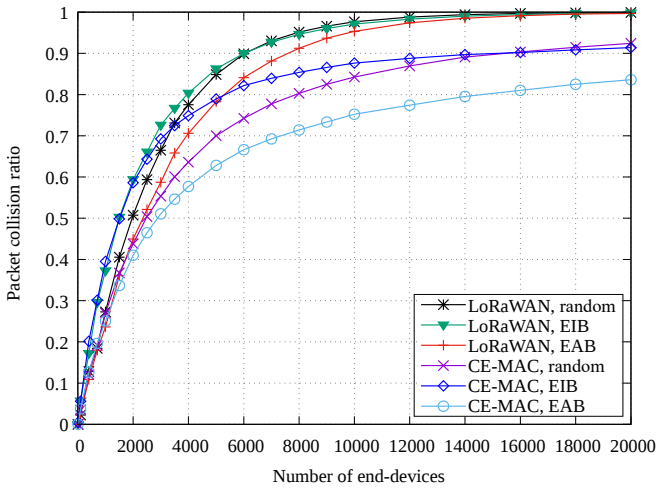

Fig. 13. Throughput rate of LoRaWAN and CE-MAC in three SF allocation schemes.

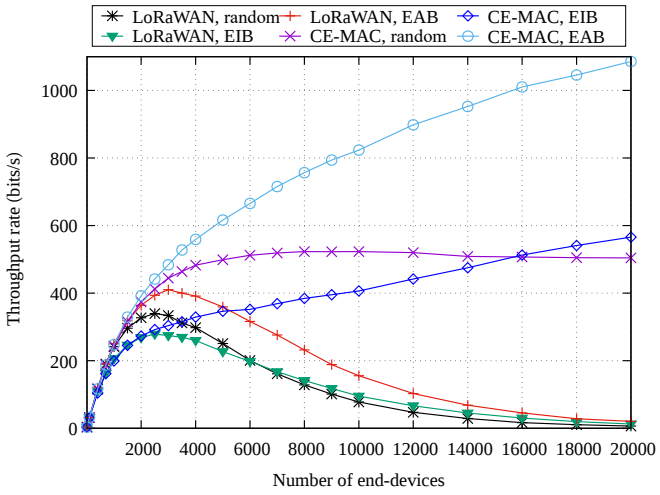

Fig. 14. Throughput rate of LoRaWAN and CE-MAC in three SF allocation schemes.

Figs. 13 and 14 show the PCR and throughput rates of LoRaWAN with capture effect and the CE-MAC protocol, respectively. For the same SF allocation scheme, the CE-MAC protocol has a lower PCR and higher throughput rate due to the fact that the CE-MAC protocol can better exploit capture effect to resolve collisions. For the same protocol, the EAB scheme has the best performance. This is because the end-devices near the gateway have the smaller SFs and those far from the gateway have the bigger SFs. In this way, more packets in the EAB scheme can fulfill the SINR threshold required for demodulation. The EIB scheme works worse than the random scheme when the number of end-devices is small, but outperforms the random scheme when the number of end-devices scales up. Because the area of big SF in the EIB scheme is larger, more packets possess a long ToA and the network will suffer from more collisions and congestions. While as the number of end-devices grows, more packets can satisfy the capture condition in the EIB scheme than the random scheme, which results in a performance ehancement. Consequently, the proposed CE-MAC protocol shows a potential for smart city and other mIoT applications.

VI. CONCLUSIONS

This paper proposed CE-MAC, a novel MAC protocol exploiting the concurrent transmissions and the LoRa capture effect that provides support for massive connectivity in IoT. For this purpose, a novel LoRa receiver structure using oversampling was firstly designed, which was able to decode superposed signals with different odd/even SFs simultaneously. Then the CE-MAC protocol based on the novel receiver structure was proposed. The end-devices in the CE-MAC protocol could transmit frames concurrently and both the co-SF and the inter-SF collisions could be reduced through exploiting the capture effect. Simulations verified that, the CE-MAC protocol significantly outperformed the conventional LoRaWAN in terms of the collision ratio and the network throughput even with a number of end-devices up to 2×10^4. The efficient features indicate the proposed scheme is superior to LoRaWAN for fulfilling the massive connectivity in the LoRa IoT networks.

REFERENCES

[1] U. Raza, P. Kulkarni, and M. Sooriyabandara, "Low power wide area networks: An overview," *IEEE Commun. Surveys Tuts.*, vol. 19, no. 2, pp. 855–873, 2017.

[2] L. Vangelista, A. Zanella, and M. Zorzi, "Long-range IoT technologies: The dawn of LoRa," *Springer, Cham. Future Access Enablers for Ubiquitous Intelligent Infrastructures*, vol. 159. pp. 51–59, Sept. 2015.

[3] "LoRaWAN 1.1 Specification," LoRa Alliance, Inc., Brandin Court Fremont, CA, USA, Oct. 2017, pp. 1–101. [Online]. Available: https://lora-alliance.org/resource-hub/lorawanr-specification-v11

[4] M. Shirvanimoghaddam, M. Dohler, and S. J. Johnson, "Massive non-orthogonal multiple access for cellular IoT: Potentials and limitations," *IEEE Commun. Mag.*, vol. 55, no. 9, pp. 55–61, Sept. 2017.

[5] Z. Chen, F. Sohrabi, and W. Yu, "Sparse activity detection for massive connectivity," *IEEE Trans. Signal Process.*, vol. 66, no. 7, pp. 1890–1904, Apr. 2018.

[6] L. Liu and W. Yu, "Massive connectivity with massive MIMO–part I: Device activity detection and channel estimation," *IEEE Trans. Signal Process.*, vol. 66, no. 11, pp. 2933–2946, June 2018.

[7] L. Liu and W. Yu, "Massive connectivity with massive MIMO–part II: Achievable rate characterization," *IEEE Trans. Signal Process.*, vol. 66, no. 11, pp. 2947–2959, June 2018.

[8] R. Deng, S. Zhou, and Z. Niu, "Scalable non-orthogonal pilot design for massive MIMO systems with massive connectivity," in *Proc. IEEE GlobeCom Wkshps*, Dec. 2016.

[9] M. Mohammadkarimi, M. A. Raza, and O. A. Dobre, "Signature based non-orthogonal massive multiple access for future wireless networks: Uplink Massive Connectivity for Machine-Type Communications," *IEEE Veh. Technol. Mag.*, vol. 13, no. 4, pp. 40–50, Oct. 2018.

[10] T.-Y. Chan, *et al.*, "Multi-slot allocation protocols for massive IoT devices with small-size uploading data," *IEEE Wireless Commun. Lett.*, vol. 8, no. 2, pp. 448–451, Oct. 2019.

[11] C. Bockelmann, *et al.*, "Towards massive connectivity support for scalable mMTC communications in 5G networks," *IEEE Access*, vol. 6, pp. 28969–28992, June 2018.

[12] J. Zou, *et al.*, "Packet-based preamble design for random access in massive IoT communication systems," *IEEE Access*, vol. 5, pp. 11759–11767, July 2017.

[13] L. Liu, *et al.*, "Sparse signal processing for grant-free massive connectivity: A future paradigm for random access protocols in the Internet of Things," *IEEE Signal Process. Mag.*, vol. 35, no. 5, pp. 88–99, Aug. 2018.

[14] A. Waret, *et al.*, "LoRa throughput analysis with imperfect spreading factor orthogonality," *IEEE Wireless Commun. Lett.*, vol. 8, no. 2, pp. 408–411, Apr. 2019.

[15] O. Georgiou and U. Raza, "Low power wide area network analysis: Can LoRa scale?" *IEEE Wireless Commun. Lett.*, vol. 6, no. 2, pp. 162–165, Apr. 2017.

[16] A. I. Pop, *et al.*, "Does bidirectional traffic do more harm than good in LoRaWAN based LPWA networks?" in *Proc. IEEE GLOBECOM*, Dec. 2017.
[17] C. Liao, *et al.*, "Multi-hop LoRa networks enabled by concurrent transmission," *IEEE Access*, vol. 5, pp. 21430–21446, Oct. 2017.
[18] U. Noreen, L. Clavier, and A. Bounceur, "LoRa-like CSS-based PHY layer, capture effect and serial interference cancellation," in *Proc. VDE European Wireless*, June 2018.
[19] C. Goursaud and J.-M. Gorce, "Dedicated networks for IoT: PHY/MAC state of the art and challenges," *EAI Endorsed Trans. Internet Things*, vol. 1, no. 1, pp. 1–11, Nov. 2015.
[20] T. Elshabrawy and J. Robert, "Analysis of BER and coverage performance of LoRa modulation under same spreading factor interference," in *Proc. IEEE PIMRC*, 2018, pp. 1–6.
[21] D. Croce, *et al.*, "Impact of LoRa imperfect orthogonality: Analysis of link-Level performance," *IEEE Commun. Lett.*, vol. 22, no. 4, pp. 796–799, Apr. 2018.
[22] A. Mahmood, E. Sisinni, and L. Guntupalli, "Scalability analysis of a LoRa network under imperfect orthogonality," *IEEE Trans. Ind. Informat.*, vol. 15, no. 3, pp. 1425–1436, Mar. 2019.
[23] J. C. Liando, *et al.*, "Known and unknown facts of LoRa: Experiences from a large-scale measurement study," *ACM Trans. Sensor Netw.*, vol. 15, no. 2, pp. 16–41, Feb. 2019.
[24] J.-T. Lim and Y. Han, "Spreading factor allocation for massive connectivity in LoRa systems," *IEEE Commun. Lett.*, vol. 22, no. 4, pp. 800–803, Apr. 2018.
[25] B. Reynders, *et al.*, "Improving reliability and scalability of LoRaWANs through lightweight scheduling," *IEEE Internet Things J.*, vol. 5, no. 3, pp. 1830–1842, June 2018.
[26] N. E. Rachkidy, A. Guitton, and M. Kaneko, "Collision resolution protocol for delay and energy efficient LoRa networks," *IEEE Trans. Green Commun. Netw.*, vol. 3, no. 2, pp. 535–551, June 2019.
[27] T.-H. To, A. Duda, "Simulation of LoRa in NS-3: Improving LoRa performance with CSMA," in *Proc. IEEE ICC*, May 2018.
[28] J. Ortín, M. Cesana, and A. Redondi, "Augmenting LoRaWAN performance with listen before talk," *IEEE Trans. Wireless Commun.*, vol. 18, no. 6, pp. 3113–3128, June 2019.
[29] L. Leonardi, *et al.*, "A novel medium access strategy for LoRa in industry 4.0 applications," in *Proc. IEEE IECON*, Oct. 2018.
[30] "AN1200.22 LoRa modulation basis," Semtech Corporat., Application Note Revision 2, Camarillo, CA, USA, May. 2015, pp. 1–26. [Online]. Available: https://www.semtech.com/uploads/documents/an1200.22.pdf
[31] T. Elshabrawy and J. Robert, "Closed-form approximation of LoRa modulation BER performance," *IEEE Commun. Lett.*, vol. 22, no. 9, pp. 1778–1781, Sept. 2018.
[32] T. Elshabrawy and J. Robert, "Interleaved chirp spreading LoRa-based modulation," *IEEE Internet Things J.*, vol. 6, no. 2, pp. 3855–3863, Apr. 2019.
[33] L. Vangelista, "Frequency shift chirp modulation: The LoRa modulation," *IEEE Signal Process. Lett.*, vol. 24, no. 12, pp. 1818–1821, Dec. 2017.
[34] B. Dunlop, *et al.*, "Interference analysis for LoRa chirp spread spectrum signals," in *Proc. IEEE CCECE*, May 2019.
[35] "SX1301 datasheet," Semtech Corporat., Wireless and Sensing Products V2.4, Camarillo, CA, USA, June 2017, pp. 1–40. [Online]. Available: https://www.semtech.com/uploads/documents/sx1301.pdf
[36] A. Hoeller, *et al.*, "Analysis and performance optimization of LoRa networks with time and antenna diversity," *IEEE Access*, vol. 6, pp. 32820–32829, July 2018.
[37] J. Petajajarvi, *et al.*, "On the coverage of LPWANs: Range evaluation and channel attenuation model for LoRa technology," in *Proc. IEEE ITST*, Dec. 2015.
[38] "LoRaWAN 1.1 regional parameters," LoRa Alliance, Inc., Brandin Court Fremont, CA, USA, Jan. 2018, pp. 1–72. [Online]. Available: https://lora-alliance.org/resource-hub/lorawanr-regional-parameters-v11rb
[39] A. Zanella, *et al.*, "Internet of things for smart cities," *IEEE Internet Things J.*, vol. 1, no. 1, pp. 22–32, Feb. 2014.
[40] M. Centenaro, *et al.*, "Long-range communications in unlicensed bands: The rising stars in the IoT and smart city scenarios," *IEEE Wireless Commun.*, vol. 23, no. 5, pp. 60–67, Oct. 2016.
[41] "Cellular system support for ultra-low complexity and low throughput internet of things (CIoT)," 3GPP Standard TR 45.820, Nov. 2015.

Yujun Hou received the B.S. degree from Xidian University, Xi'an, China, in 2017. He is currently pursuing his M.S. degree in Electronic and Telecommunications Engineering at the State Key Laboratory of Integrated Services Networks, Xidian University. His research interests include physical and MAC layer techniques for LoRa.

Zujun Liu received the B.S., M.S., and Ph.D. degrees from Xi'an Jiaotong University, Xi'an, China, in 1998, 2001, and 2006, respectively. From 2001 to 2002, he was a Hardware Engineer with ZTE Ltd. He joined Xidian University, China, in 2006, as a Lecturer, where he is currently a Professor with the State Key Laboratory of Integrated Services Networks. His current research interests are interference management for wireless communications, radio resource allocation, and the Internet of Things.

Dechun Sun received the B.S., M.S. and Ph.D. degrees from Xidian University, Xi'an, China, in 2003, 2006 and 2012 respectively, all in Telecommunications Engineering. Since then, he has been in the Department of Telecommunications Engineering, Xidian University, Xi'an, China, where he is currently an Associate Professor. His research interests include signal processing, wireless communications, and satellite communications.